International Research Journal on Advanced Engineering Hub (IRJAEH)
e ISSN: 2584-2137
Vol. 03 Issue: 09 September 2025
Page No: 3464-3471
https://irjaeh.com
https://doi.org/10.47392/IRJAEH.2025.0509

A Metamaterial Inspired Antenna for Sub 6GHZ 5G Application

Harshavardhan Reddy[1], Dr. Rajendra R Patil[2]
[1]Department of Electronics and Communication Engineering, Faculty of Engineering and Technology, Sharnbasva University, Kalaburagi-585103, Karnataka, India
[2]Department of Electronics and Communication Engineering, GSSS Institute of Engineering and Technology for Women – Mysuru-570016, Karnataka, India (Affiliated to Visvesvaraya Technological University, Belagavi.)
Emails: harshareddy86@gmail.com[1], rajendra.nano@gmail.com[2]

Abstract
The study examines a small, low-profile, metamaterial inspired antenna for sub-6 GHz 5G applications that is loaded with a circular complementary split ring resonator (C-CSRR) based on negative permittivity and permeability. Two popular frequency bands, n78 5G NR and n79 5G NR (2.78–7.03) GHz, are produced by adding metamaterial to the radiator. The corresponding gains are 6.24 dB and 5.3 dB. The design is able to achieve high impedance bandwidth of 4.25 GHz from 2.78GHz to 7.03GHz with high return loss (S11 <-37 dB). The antenna offers simulated radiation efficiency of 96.09% at 3.5 GHz and 93.41% at 6.45 GHz making it suitable for 5G communication demands. The antenna constructed on a FR-4 substrate with a dielectric constant of 4.4 and measures just 28 x 28 x 1.6 mm3. HFSS simulation software is being put into use to design, model, and measure the suggested antenna parameters in a real-world environment. The simulated outcome demonstrates that the suggested metamaterial antenna's peak gain is around 6dB to 7 dB and it has a resonance frequency for C-band applications, including weather radar systems and 5G applications.
Keywords: *5G, CSRR, Metamaterial, Radar, Wideband.*

1. Introduction
The development of 5G technology has sparked interest among researchers in creating innovative antennas with special wireless communication features. The market for antennas is growing as digitization becomes the norm. There is a need for high bandwidth, high data rate, and low latency when billions of devices are online [1]. Although millimeter waves are the best option for handling huge volumes of data because they match the requirements of high bandwidth, high data rate, and high connection density, they are susceptible to free space loss and require specialized equipment to counteract the loss [2]. The cost of installing 5G technology is quite high since it requires more advanced equipment to prevent losses. Thus, the quick fix to satisfy consumer demand for 5G technologies is to change to midband millimeter wave, sometimes referred to as sub-6 GHz [3]. Researchers are particularly interested in two sub-6 GHz frequency bands: n79 5G NR (4.98–6.19) and 78 5G NR (3.13–4.01) GHz. The traditional cellular system has evolved into what we see today. These are incorporated into telemedicine, the internet of things (IOT), driverless cars, smart homes, and smart cities. Since the manufacturers favor small, portable devices, these applications require low profile, compact, high directivity antennas to eliminate space limitations [4]. In recent years, metamaterial structures have emerged as a promising option for antenna integration. The structural parameter, not the material, is what causes the metamaterial property. Over the past few decades, a lot of work has advanced and new structures have emerged. Metamaterial-inspired antennas, particularly those utilizing complementary split-ring resonators (CSRRs), have attracted significant attention for compact multiband

International Research Journal on Advanced Engineering Hub (IRJAEH)
e ISSN: 2584-2137
Vol. 03 Issue: 09 September 2025
Page No: 3464-3471
https://irjaeh.com
https://doi.org/10.47392/IRJAEH.2025.0509

wireless communication systems. A small tri-band antenna based on hexa-complementary split-ring resonators (HCSRRs) has been proposed for 4G communication, achieving coverage of WLAN, WiMAX, and Wi-Fi bands by carefully optimizing the resonator's dimensions and positioning [5]. Similarly, studies have demonstrated that integrating hexagonal CSRR slots into monopole antennas enhances multiband behavior, with the passband characteristics of HCSRRs playing a critical role in performance evaluation [6]. Further advancements include etching modified CSRRs onto the ground plane to create permeable bands that support multiple resonant frequencies [7], while splitting the outer hexagonal ring of CSRRs has been shown to significantly improve bandwidth [8]. With the transition to 5G, metamaterial antennas have been integrated into distributed antenna systems (IDAS), operating effectively in the 3.5–6 GHz range through novel combinations of rectangular and triangular patch elements with CSRR unit cells [9]. Other designs have utilized trapezoidal radiating patches with triangular CSRRs, where different structural loadings yield multiple resonant frequencies [10]. CSRR-based metamaterials have also been applied to improve isolation in antenna arrays, demonstrating their ability to achieve high quality factors at microwave frequencies [11]. In MIMO systems, metamaterial-inspired fractal antennas employing CSRRs have achieved ultra-wideband impedance bandwidths (5.8–15 GHz) while reducing mutual coupling below –25 dB [12]. Additionally, compact CSRR-loaded antennas have reported excellent results at 2.4 GHz, including a return loss of –46.58 dB, a 574 MHz bandwidth, and a gain of 3.23 dBi [13]. Recent studies extend these concepts into mm-wave and specialized applications. A dual-band filtering antenna for automotive 5G employed square CSRRs with inter-digital lines to generate radiation nulls, maintaining a stable 4.3 dBi gain across the 26.5–29.5 GHz and 37–43.5 GHz bands [14]. Miniaturization approaches include T-shaped CSRR (T-CSRR) antennas, achieving resonance at 2.45 GHz within a 0.14λ × 0.26λ footprint, further enhanced to 9 dBi in a 1×4 array configuration [15]. For GSM and WiMAX/WLAN, CSRR-loaded monopoles have demonstrated dual- and tri-band performance with high return loss and gain [16]. Similarly, quad-band fractal monopoles with CSRR-backed ground planes have provided wideband functionality through geometric fractal effects [17]. Advanced metamaterial techniques such as composite right/left-handed transmission lines (CRLH-TL) have enabled dual-band SRR–CSRR–SIW antennas with gains above 5.3 dBi [18]. Circular polarization and size reduction were realized using complementary slotted SRRs, achieving 61% miniaturization and robust axial ratio bandwidth [19].

2. Method

The development of the proposed antenna is displayed in Fig. 1 (a–c). First a simple hexagonal monopole antenna is designed with a resonance frequency according to Eq.1 [20].

$$f_r = \frac{1.8412c}{2\pi S\varepsilon_r} = \frac{1.8412\ x\ 3\ x\ 10^8}{2\pi\ x\ 9\ x\ 10^{-3}\sqrt{4.4}} = 4.7GHz \quad (1)$$

Here, S is the hexagonal monopole radiator's side length and c is the speed of light. The relative dielectric constant is denoted by ε_r. Utilizing partial ground and microstrip feeding 3.88 GHz is the frequency at which the parent antenna resonates. Next, a single circular CSRR with an inner radius of 2 mm and an outer radius of 3 mm is added to the patch's middle portion, with a slit gap of 0.3 mm. Due to the increased capacitance effect introduced by the slot, the resonance frequency is shifted to a lower frequency. This changes the current distribution and establishing a new resonance. Electric resonance enables wideband radiation to be achieved by the suggested CSRR.Next, a 4 mm-radius circle is sliced vertically on both sides of the hexagonal monopole to create a guitar shape, which reduces surface volume and aiding in the decrease of size. The existing path is also made longer by the size reduction. Table 1 lists the proposed antenna's dimensions, while Fig. 1(c) shows a graphical depiction of its structure. Figure 1 Shows Conventional Antenna Figure 2 Shows Antenna with CSRR, Figure 3 Shows Antenna with

International Research Journal on Advanced Engineering Hub (IRJAEH)
e ISSN: 2584-2137
Vol. 03 Issue: 09 September 2025
Page No: 3464-3471
https://irjaeh.com
https://doi.org/10.47392/IRJAEH.2025.0509

CSRR & Slice Table 1 shows Dimensions of the Proposed Antenna

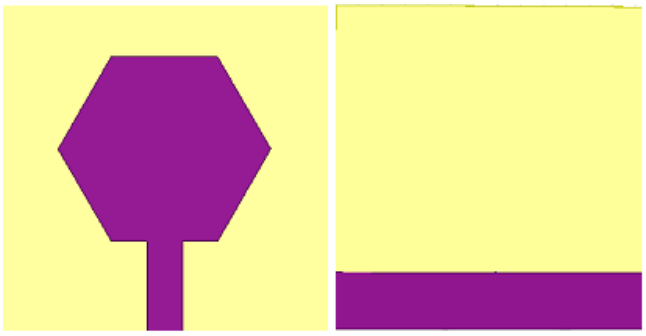

Figure 1 Conventional Antenna

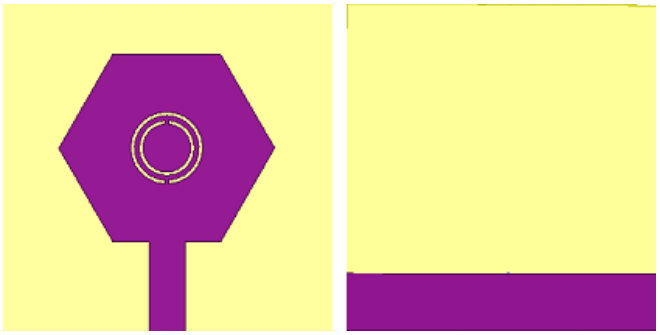

Figure 2 Antenna with CSRR

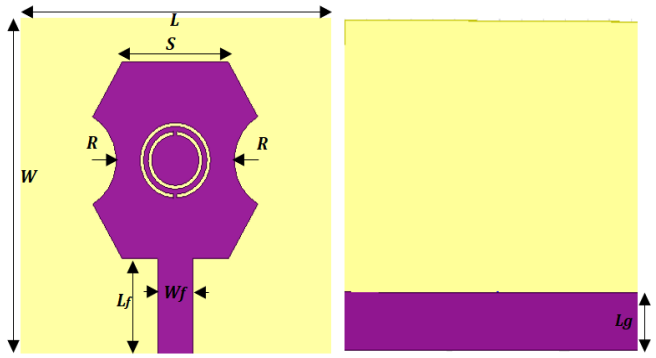

Figure 3 Antenna with CSRR & Slice

Figure 2 depicts the CSRR structure and its inherent equivalent circuit model. This analogous circuit is made up of two parallel inductors, each of which is represented by L0/2 and connects the disc to ground, as well as a capacitance, CCSRR, that is made up of a disc with a radius of r0-c/2 that is encircled by a ground plane. Figure 4 shows LC Circuit with Its Identical CSRR Structure

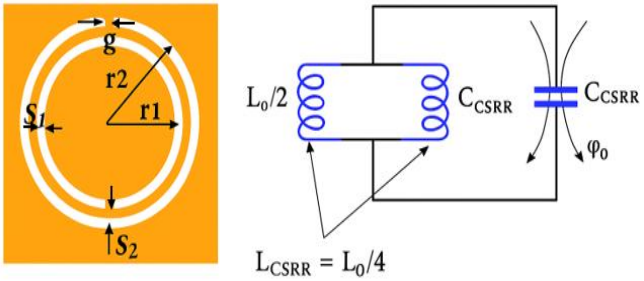

Figure 4 LC Circuit with Its Identical CSRR Structure

Table 1 Dimensions of the Proposed Antenna

Antenna parameters	Dimensions in mm
L	28
W	28
R	4
S	9
Lf	7.8
Wf	3
Lg	4.9
S1	0.3
S2	0.4
r1	2
r2	3
g	0.3

The LC tank circuit diagram shown in Figure 2 determines the circular CSRR's resonance frequency. The circular complementary split ring resonator (C-CSRR's) slit gap is crucial for generating pass band behavior. The inductance effect (L_{CSRR}) is caused by the slit along the slot, and the capacitance effect (C_{CSRR}) is caused by the slot along the slit. The CSRR inductance (L_{CSRR}) is caused by the copper strip within the slots, whereas the capacitance (C_{CSRR}) is caused by the gap across the copper strips. SRR and CSRR are regulated by the same expression when using babinet principle. Therefore, the CCSRR resonance frequency is calculated by:

$$f_{CSRR} = \frac{1}{2\pi\sqrt{L_{CSRR}C_{CSRR}}} \quad (2)$$

International Research Journal on Advanced Engineering Hub (IRJAEH)
e ISSN: 2584-2137
Vol. 03 Issue: 09 September 2025
Page No: 3464-3471
https://irjaeh.com
https://doi.org/10.47392/IRJAEH.2025.0509

Where,

$$C_{CSRR} = \frac{N-1}{2}[2L - (2N-1)(W+S)]C_0 \quad (3)$$

$$C_0 = \varepsilon_0 \frac{K(\sqrt{1-K^2})}{K(k)} \text{ and } k = \frac{\frac{S}{2}}{W+\frac{S}{2}} \quad (4)$$

$$L_{CSRR} = 4\mu 0[L-(N-1)(S+W)]\left[ln\left(\frac{0.98}{\rho}\right) + 1.84\rho\right] \quad (5)$$

$$\rho = \frac{(N-1)(S+W)}{1-(N-1)(W+S)} \quad (6)$$

The first order elliptic integral K(k) is denoted as K, while N is the number of circular CSRR slots, R in equation is the CSRR's radius, W (g) is the CSRR's slot width, and S (S1) is the distance between the CSRR slots. When calculating quasi-static capacitance, especially when using conformal mapping techniques for planar transmission lines or resonator structures, the ratio in equation.4 appears in a standard form. This dimensionless elliptic integral solely depends on the modulus k, which is determined by geometrical parameters (spacing S1 and slot width W(g)) in this antenna design.

3. Results And Discussion

3.1 Results

ANSYS HFSS simulation software version 15 is used for all the simulations. All of the proposed antenna's properties, including radiation pattern, return loss, bandwidth and size reduction were investigated through simulation. The statistics clearly show that the resonant frequency was significantly decreased by carving a circular CSRR on the radiating plane and adding a slice to the radiating patch, which resulted in a reduction in size. The circular CSRR has enhanced the bandwidths of the antennas. Furthermore, every antenna that has been shown has a large bandwidth. The Figure 3 demonstrates the simulated return loss for various proposed antennas discussed in fig.1. It is observed that the introduction of CSRR decreases the resonant frequency to the desired frequency and the introduction of slice on both sides of patch increases the return loss S11 of the antenna also upgrading the antenna with wide bandwidth. Figure 5 shows Return loss all Proposed antennas

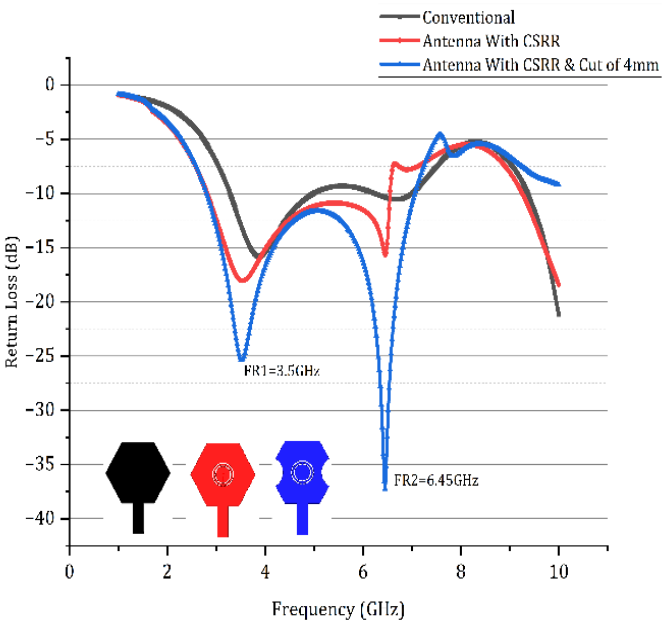

Figure 5 Return Loss All Proposed Antennas

The Figure 4 demonstrates the simulated return loss for various antennas whose radius of slice R is varied in between 2.5 mm to 4.5 mm, the gap between the two rings (S1 & S2) is kept constant. Here it is observed that the ideal return loss for the desired application is obtained at R=4mm, and the antenna with 4mm radius slice with circular CSRR is etched on radiating element to increase the bandwidth and resonate at desired frequencies. This also demonstrates the wider bandwidth is achieved as R increases, particularly noticeable around the second resonance. The projected multiband antenna's simulated gain is seen in the Figure 5, i.e. 6.24 dB for frequency 3.5 GHz. Sometimes the gain pattern is also known as the gain at function direction plot. With the help of the HFSS application, the gain is shown in a 3D polar plot. The gain of the antenna enhanced and examined in contrast to other designs by incorporating a reflector, DGS, and parasitic elements Figure 6 shows Return Loss of Antennas with Different Values of R (Slice Radius) Figure 7 shows Gain of Proposed Antenna at 3.5GHz

International Research Journal on Advanced Engineering Hub (IRJAEH)
e ISSN: 2584-2137
Vol. 03 Issue: 09 September 2025
Page No: 3464-3471
https://irjaeh.com
https://doi.org/10.47392/IRJAEH.2025.0509

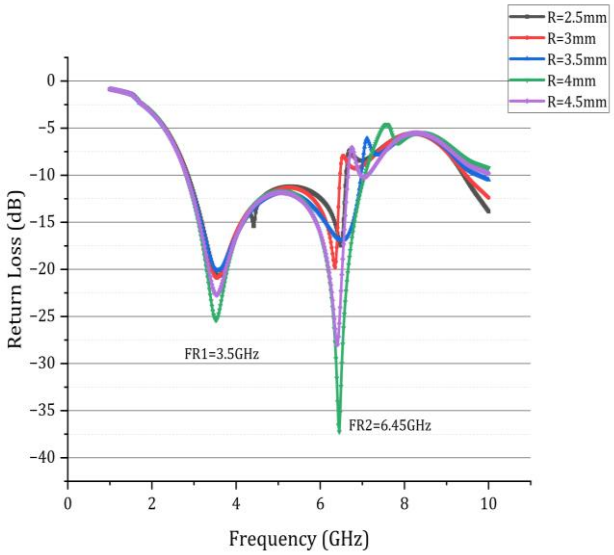

Figure 6 Return Loss of Antennas with Different Values of R (Slice Radius)

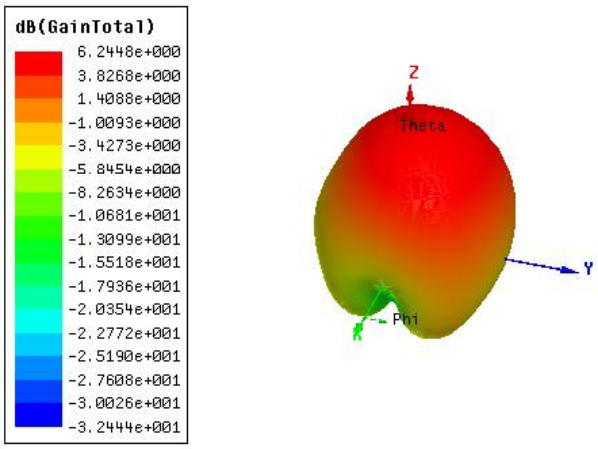

Figure 7 Gain of Proposed Antenna at 3.5GHz

the azimuth and elevation angles of the antenna, is the strength of the radio waves emitted from the antenna in different directions. Every antenna should have zero near-end radiation and a fan-shaped radiation pattern at the far end. The radiation pattern at frequencies of 3.5 GHz, 8.15 GHz, and 6.45 GHz at ^{y}=0 and ^{y}=90 degrees has been examined using the HFSS program and is shown in the figure.8. The power is sent to the far end of the assigned antenna using azimuth and elevation angle. Figure 8 shows Radiation Pattern at 3.5GHz, Figure 9 shows Radiation Pattern at 6.45 GHz

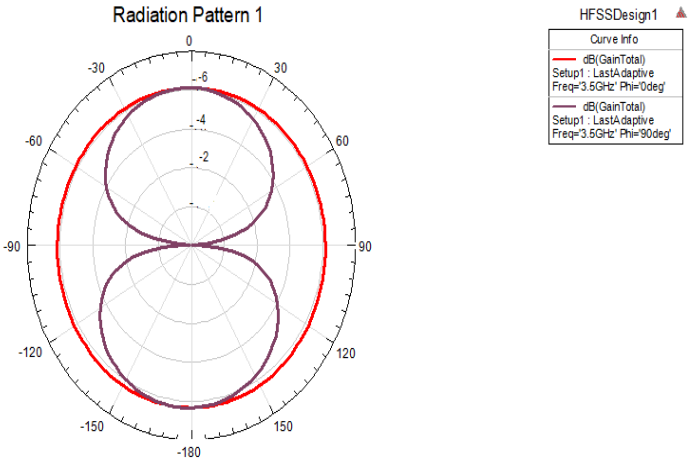

Figure 8 Radiation Pattern at 3.5GHz

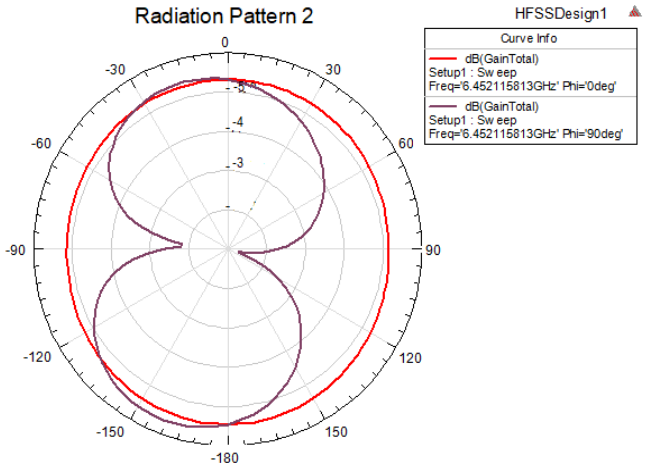

Figure 9 Radiation Pattern at 6.45 GHz

Figure &. illustrates the simulated surface current distribution on a patch antenna using C-CSRR; Figure 7(a) shows the spread at 3.5 GHz, while Figure 7(b) shows it at 6.45 GHz. The image's surface current distribution demonstrates the performance advantages that come with adding a CSRR to the antenna construction. Effective excitation of the antenna is confirmed by the high current density surrounding the feedline and coupling region on the left side of the picture. The CSRR slot's resonance at the intended frequency is confirmed by the significant surface current localization around it on the right. Figure 10 shows Surface Current Distribution on Patch Surface Current at 3.5 GHz, Figure 11 Surface shows Current Distribution on Patch Surface Current at 6.45 GHz

International Research Journal on Advanced Engineering Hub (IRJAEH)
e ISSN: 2584-2137
Vol. 03 Issue: 09 September 2025
Page No: 3464-3471
https://irjaeh.com
https://doi.org/10.47392/IRJAEH.2025.0509

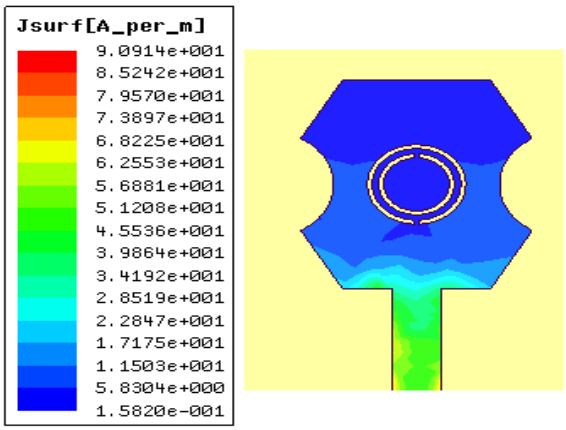

Figure 10 Surface Current Distribution on Patch Surface Current at 3.5 GHz

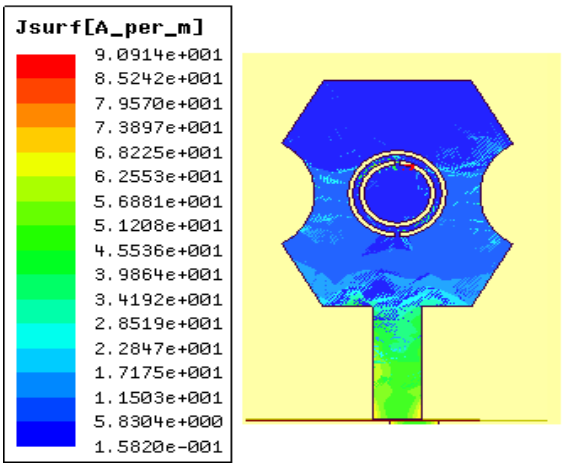

Figure 11 Surface Current Distribution on Patch Surface Current at 6.45 GHz

4. Discussion

The comparative performance of the developed antennas is summarized in Table 2. The conventional antenna resonates at 3.88 GHz with a return loss of –15.89 dB, a bandwidth of 1.8 GHz, and a gain of 2.1 dB. By incorporating the complementary concentric split ring resonator (CCSRR), the antenna exhibits dual-band operation at 3.5 GHz and 6.45 GHz, with improved return loss values of –18.2 dB and –15.66 dB, respectively. In addition, the bandwidth increases to 3.4 GHz, and the gain is enhanced to 3.45 dB. Further improvement is observed when both the CCSRR and slice are introduced, as the antenna achieves dual resonances at 3.5 GHz and 6.5 GHz with significantly better return loss of –25.3 dB and –37.22 dB. The bandwidth also increases to 4.25 GHz, while the gain reaches a maximum of 6.24 dB. These results clearly demonstrate that the inclusion of CCSRR and slicing techniques substantially improves the impedance matching, bandwidth, and radiation characteristics of the antenna compared to the conventional design Table 2 shows Comparison Between Conventional Antenna and Proposed Antennas

Table 2 Comparison Between Conventional Antenna and Proposed Antennas

Developed antenna	Resonant Frequency in GHz	Return loss in dB	Band width in GHz	Gain in dB
Conventional	3.88	-15.89	1.8	2.1dB
Antenna with CCSRR	3.5 & 6.45	-18.2, -15.66	3.4	3.45dB
Antenna with CCSRR and Slice	3.5 & 6.5	-25.3, -37.22	4.25	6.24dB

The performance of our suggested Metamaterial antenna is compared to several previously published attempts in Table 3. The works are arranged based on a number of factors, including the size, frequency range, bandwidth, and gain of the antenna. High gain, bandwidth, and return loss are among the remarkable features of the proposed Metamaterial antenna, according to the comparing process. Table 3 shows Comparison with Previous Work

Table 3 Comparison with Previous Work

Ref. Number	Dimensions (mm x mm)	Resonant Frequency In GHz	Bandwidth in MHz	Gain
[5]	45 x 45	2.45, 2.86, 6.19	180, 150, 420	3.16
[8]	30 x 30	2.4, 4.64	180, 2400	4.6
[11]	25 x 25	2.4, 5.2, 7.4, 8.2	220, 90, 110,100	1.22
[15]	20 x 34 x 1.6	1.83, 3.65, 5.59	120, 3132	3.16
[17]	24.5×30×0.508	5.26, 9.11	3,12	5.33
Proposed	28 x 28 x 1.6	3.5, 6.45	4.25 GHz	6.24

International Research Journal on Advanced Engineering Hub (IRJAEH)
e ISSN: 2584-2137
Vol. 03 Issue: 09 September 2025
Page No: 3464-3471
https://irjaeh.com
https://doi.org/10.47392/IRJAEH.2025.0509

Conclusion

The proposed antenna design demonstrates significant improvements in bandwidth, return loss, and gain compared to the conventional structure. By integrating CCSRR and slicing techniques, the antenna achieves dual-band operation at 3.5 GHz and 6.5 GHz with enhanced impedance matching and radiation characteristics. These features make the antenna a strong candidate for modern wireless communication systems, particularly for 5G applications operating in sub-6 GHz covering the n78 and n79 bands with peak gains up to 6 dB and efficiencies above 96%, the antenna ensures reliable operation for 5G communication as well as C-band applications such as weather radar systems.

References

[1]. J.G. Andrews et al., What Will 5G Be?, IEEE J. Select. Areas Commun. 32 (2014) 1065 doi: 10.1109/JSAC.2014.2328098.

[2]. X. Tong, Z. H. Jiang, C. Yu, F. Wu, X. Xu, W. Hong, Lowprofile, broadband, dual-linearly-polarized, and wide-angle millimeter-wave antenna arrays for Ka-Band 5G applications, in: IEEE Antennas and Wireless Propagation Letters (2021)3102375. doi:10.1109/LAWP.2021.3102375.

[3]. W. Roh et al., Millimeter-wave beamforming as an enabling technology for 5G cellular communications: theoretical feasibility and prototype results, IEEE Commun. Mag. 52 (2014) 106 doi: 10.1109/ MCOM. 2014. 6736750.

[4]. Farasat, Madiha, Dushmantha N. Thalakotuna, Zhonghao Hu, Yang Yang, A review on 5G Sub-6 GHz base station antenna design challenges, Electronics 2000 10 (2021) 16. https:// doi.org/ 10.3390/ electronics10162000

[5]. Aminu-Baba, Murtala, Mohamad Kamal A. Rahim, Farid Zubir, Mohd Fairus Mohd Yusoff, Adamu Y. Iliyasu, Mohammed Mustapha Gajibo, Huda A. Majid, and K. I. Jahun. 2020. "A compact triband microstrip antenna utilizing hexagonal CSRR for wireless communication systems." Bulletin of Electrical Engineering and Informatics 9 (5): 1916–23. https:// doi.org/ 10.11591/ eei.v9i5. 2191.

[6]. Daniel, R. Samson, R. Pandeeswari, and S. Raghavan. 2018. "A miniaturized printed monopole antenna loaded with hexagonal complementary split ring resonators for multiband operations." International Journal of RF and Microwave Computer-Aided Engineering 28 (7): 1–8. https://doi.org/10.1002/mmce.21401.

[7]. Manikandan, Palanivel, Pothiraj Sivakumar, and Nagarajan Rajini. 2022. "Multi-band Antenna with CSRR Loaded Ground Plane and Stubs Incorporated Patch for WiMAX/WLAN Applications." Pertanika Journal of Science and Technology 30 (1): 35–52. https:// doi.org/ 10.47836/ PJST. 30.1.03.

[8]. Murugeshwari, B., R. Samson Daniel, and S. Raghavan. 2019. "A compact dual band antenna based on metamaterial-inspired split ring structure and hexagonal complementary split-ring resonator for ISM/WiMAX/WLAN applications." Applied Physics A: Materials Science and Processing 125 (9): 1–8. https://doi.org/10.1007/s00339-019-2925-x.

[9]. Karimbu Vallappil, Arshad, Bilal A. Khawaja, Mohamad Kamal A. Rahim, Muhammad Naeem Iqbal, and Hassan T. Chattha. 2022. "Metamaterial-Inspired Electrically Compact Triangular Antennas Loaded with CSRR and 3 × 3 Cross-Slots for 5G Indoor Distributed Antenna Systems." Micromachines 13 (2). https:// doi.org/ 10.3390/mi13020198

[10]. Yeo, Junho, and Jong Ig Lee. 2020. "Design of a high-sensitivity microstrip patch sensor antenna loaded with a defected ground structure based on a complementary split ring resonator." Sensors (Switzerland) 20 (24): 1–18. https://doi.org/10.3390/s20247064

[11]. Rajkumar, Rengasamy, and Usha Kiran Kommuri. 2018. "A Triangular Complementary Split Ring Resonator Based

International Research Journal on Advanced Engineering Hub (IRJAEH)
e ISSN: 2584-2137
Vol. 03 Issue: 09 September 2025
Page No: 3464-3471
https://irjaeh.com
https://doi.org/10.47392/IRJAEH.2025.0509

Compact Metamaterial Antenna for Multiband Operation." Wireless Personal Communications 101 (2): 1075–89. https://doi.org/10.1007/s11277-018-5749-7.

[12]. Reddy, Mekala Harinath, D. Sheela, Vinay Kumar Parbot, and Abhay Sharma. 2021. "A compact metamaterial inspired UWB-MIMO fractal antenna with reduced mutual coupling." Microsystem Technologies 27 (5): 1971–83. https://doi.org/10.1007/s00542-020-05024-z.

[13]. Geetharamani, G., and T. Aathmanesan. 2020. "Design of Metamaterial Antenna for 2.4 GHz WiFi Applications." Wireless Personal Communications 113 (4): 2289–2300. https://doi.org/10.1007/s11277-020-07324-z.

[14]. H. Jin et al., "Compact T-CSRR antenna and antenna array," J. Electromagn. Waves Appl., vol. 35, no. 16, pp. 2193–2209, 2021.

[15]. S. Prasad Jones Christydass and N. Gunavathi, "Dual-band CSRR engraved monopole antenna," Prog.Electromagn. Res. C, vol. 113, pp. 251–263, 2021.

[16]. S. Manoharan et al., "Quad-band fractal antenna with CSRR-backed ground," Appl. Phys. A, vol. 127, 703, 2021.

[17]. L. He et al., "High-efficiency compact SRR–CSRR–SIW antenna based on CRLH-TL," J. Electromagnets. Waves Appl., vol. 35, 2021

[18]. M. S. Rao and P. I. Basarkod, Complementary slotted SRR-loaded truncated arc patch antenna," Prog. Electromagn. Res. C, vol. 101, pp. 203–218, 2020.

[19]. R. Das et al., "Analysis of Inscribed Hexagonal Slot Loaded Antenna for Short Range RFID Reader Applications," Prog. Electromagn. Res. C, vol. 150, pp. 125–133, 2024

[20]. R. Samson, Daniel Broadband m-negative antennas using ELC unit cell Int. J. Electron. Commun. (AEU¨) 118 (2020) 153147 https://doi.org/10.1016/j.aeue.2020.153147.